Comparative Study of Fuzzy Logic, P&O, Incremental Conductance, and Artificial Neural Network MPPT Methods in Fluctuating Irradiance

Kamal Boujaghama[1,*], Naoufel Khaldi[2], Rachid Markazi[1] and Lahcen Amhaimar[3]

[1] Energies and Sustainable Development Research Team (E2D), Higher School of Technology–Guelmim, Ibnou Zohr University, Guelmim, 81000, Morocco

[2] Laboratory of Electronics and Signals Treatment and Physical Modelling, Ibnou Zohr University, Agadir, 80000, Morocco

[3] DT2IA Team, M2S2I Laboratory, ENSAD, Hassan II University, Casablanca, 20000, Morocco

INFORMATION

Keywords:
MPPT
fuzzy logic
artificial neural networks
incremental conductance
perturb and observe

DOI: 10.23967/j.rimni.2025.10.71134

SCIPEDIA Revista Internacional de Métodos Numéricos para Cálculo y Diseño en Ingeniería

Revista Internacional Métodos numéricos para cálculo y diseño en ingeniería RIMNI in cooperation with CIMNE

Comparative Study of Fuzzy Logic, P&O, Incremental Conductance, and Artificial Neural Network MPPT Methods in Fluctuating Irradiance

Kamal Boujaghama[1,*], **Naoufel Khaldi**[2], **Rachid Markazi**[1] **and Lahcen Amhaimar**[3]

[1]Energies and Sustainable Development Research Team (E2D), Higher School of Technology–Guelmim, Ibnou Zohr University, Guelmim, 81000, Morocco

[2]Laboratory of Electronics and Signals Treatment and Physical Modelling, Ibnou Zohr University, Agadir, 80000, Morocco

[3]DT2IA Team, M2S2I Laboratory, ENSAD, Hassan II University, Casablanca, 20000, Morocco

ABSTRACT

Photovoltaic (PV) energy is among the renewable and clean energies which are been widely used in recent years worldwide. To ensure optimal energy extraction under dynamic irradiance and temperature conditions, improving the efficiency of PV systems requires advanced Maximum Power Point Tracking (MPPT) techniques. To identify the most suitable technique that can be implemented practically, we conduct a comparative study in this paper between MPPT algorithms, namely Incremental Conductance (INC), Perturb and Observe (P&O), Fuzzy Logic (FL), and Artificial Neural Network (ANN). Using MATLAB/Simulink, our study was conducted under the same operating conditions, with a focus on efficiency, statistical analysis of robustness, and computational complexity. Our results show that the FL controller delivered the best overall performance, whose effectiveness depends on the accuracy of the rule base and scaling factors. It is characterized by a mean efficiency of 97.17%, a rapid response of 0.0585 s, minimal steady-state oscillations, and strong adaptability to environmental variations. The ANN-based approach achieves a mean efficiency of 94.91% and exhibits high performance at medium to high irradiance levels. However, its efficiency decreases significantly at low irradiance, resulting in reduced stability and increased deviation. INC and P&O achieve mean efficiencies of 95.20% and 95.15%, respectively. Moreover, due to their low computational cost, both techniques can be easily implemented. However, under rapidly changing conditions, they exhibit slower dynamics and more pronounced oscillations around the maximum power point, resulting in less stability.

OPEN ACCESS

Received: 01/08/2025

Accepted: 14/10/2025

Published: 23/01/2026

DOI
10.23967/j.rimni.2025.10.71134

Keywords:
MPPT
fuzzy logic
artificial neural networks
incremental conductance
perturb and observe

1 Introduction

PV systems are among the most attractive and reliable renewable energy sources, due to their economical and environmental advantages [1]. These systems convert solar energy directly into electrical energy without the need for moving parts. Although PV systems are generally less efficient than some other renewable energy technologies, their performance can be significantly improved by

*Correspondence: Kamal Boujaghama (kamal.boujaghama@edu.uiz.ac.ma).

implementing MPPT techniques [2] to optimize energy extraction and maximize efficiency under varying temperature and solar irradiance conditions. The MPPT techniques of PV systems are practically realized by integrating a DC–DC boost converter [3]. The Maximum Power Point (MPP) can be determined graphically from the P-V curve of the system. According to the literature, numerous MPPT algorithms have been developed, mainly Fuzzy Logic (FL) [4,5], ANN MPPT [6], fractional open-circuit voltage (FOC) method [7], INC method [8], P&O and hill climbing method [9], and others [10,11].

Historically, FOC and hill climbing are simple methods, as they can be easily implemented in practice. Although they have wide recognition, these methods have some drawbacks, such as their limited tracking accuracy, sensitivity to rapid irradiance fluctuations, and persistent oscillations around the MPP. These disadvantages make these methods more sustainable at dynamic and real-time PV levels. On the contrary, the INC and P&O methods are relatively simple, yet they are widely used in the literature to perform standard benchmarks in MPPT research. For these reasons, we include them in our study as a consistent standard for comparison with other methods. In addition to these classical approaches, we evaluate ANN and FL controllers. Despite their greater computational complexity, they offer enhanced adaptability, stability, and efficiency even under fluctuating environmental conditions such as partial shading [12]. In such a situation, the P–V curve of the PV system exhibits multiple local maxima. Therefore, conventional techniques, rather than converging to the global MPP [13], converge to a local point. To overcome this limitation and ensure more accurate and stable tracking, we employ intelligent methods such as ANN and FL due to their ability to learn and adapt to adverse environmental conditions caused by obstacles, cloud movement, or structural shading.

Numerous MPPT algorithms have been investigated under static or overly simplified conditions in the literature, where most studies restrict their focus to either conventional techniques or intelligent approaches, such as ANN and FL. Consequently, there is a notable lack of comprehensive research on identical, highly dynamic irradiance and temperature variations that closely simulate and evaluate PV operation under real conditions for both categories of algorithms. Regarding their respective strengths and weaknesses, it is impossible to draw robust, evidence-based conclusions. To overcome this limitation, we conduct a comparative study in our paper between four MPPT algorithms, namely INC, P&O, ANN, and FL. Our study offers in-depth insights into their relative performance, including efficiency and statistical analysis of their robustness and computational complexity, for real-time PV applications.

To complete our study, which initially focused on a comparative analysis of four MPPT strategies, it is necessary to investigate their robustness under noisy measurements and varying system dynamics, as these factors can impact their effectiveness. In this regard, several studies have addressed noise resilience through denoising and intelligent protection mechanisms in relation to power electronic and grid applications. Among these studies, intelligent network–based schemes [14] and deep learning–based fault protection for meshed HVDC grids [15] have demonstrated their effectiveness in advanced denoising and improving robustness against disturbances. Although these methods are beyond the scope of this study, they highlight complementary approaches that could be integrated with MPPT controllers in future works to improve tracking reliability in noisy or highly dynamic environments.

Our paper is organized as follows: Section 2 introduces the PV module model adopted. Then, we describe in Section 3 the boost converter that interfaces the PV module with the load. Section 4 presents the four MPPT techniques, namely Artificial Neural Networks, Incremental Conductance, Fuzzy Logic, and Perturb and Observe, implemented for comparison. In Section 5, we exhibit the

simulation results obtained under dynamic irradiance profiles. Finally, in Section 6, we present the main results of our work and outline our future studies.

2 Photovoltaic Module Modeling

Among the various modeling approaches proposed in the literature, the single-diode [16] configuration has gained wide adoption because it strikes an effective balance between accuracy and simplicity. Unlike the double-diode model, which provides a more detailed representation of recombination losses but requires additional parameters and higher computational effort, the single-diode approach captures the essential nonlinear behavior of the PV cell while remaining computationally efficient and easier to implement, especially in MPPT studies. As illustrated in Fig. 1, the model consists of a photocurrent source (I_{ph}) in parallel with a nonlinear diode and a shunt resistance (R_p), all of which are connected in series with a resistance (R_s). The photocurrent source is primarily influenced by two external factors: solar irradiance and the cell's operating temperature. The main electrical characteristics of the PV panel used in this work are summarized in Table 1, which provides the parameters of the KC200GT module under standard test conditions (STC). The following equations mathematically depict the PV cell's behavior:

$$I_{ph} = (I_{sc} + a \cdot (T - T_n))\frac{G}{G_n} \tag{1}$$

$$I_0 = I_{0,n}\left(\frac{T}{T_n}\right)^3 \exp\left[\frac{q \times E_g}{n \times K}\left(\frac{1}{T_n} - \frac{1}{T}\right)\right] \tag{2}$$

$$I_{0,n} = \frac{I_{sc}}{\exp\left(\frac{V_{oc}}{nV_{th}}\right) - 1} \tag{3}$$

$$I = I_{ph} - I_0\left[\exp\left(\frac{(V + R_s \cdot I)}{n \times V_{th}}\right) - 1\right] - \frac{V + R_s \cdot I}{R_p} \tag{4}$$

I_{ph}: generated current of solar cells.

$I_{0,n}$: Nominal saturation current.

I: output current of the module PV.

R_s: solar cell's series resistance (Ω).

V: Solar module voltage (V).

G: Irradiation at STC conditions.

V_{th}: the thermal voltage $V_{th} = \frac{NsKT}{q}$.

R_p: solar cell's parallel resistance (Ω).

T: Temperature of the p-n junction (in Kelvin).

I_0: saturation current of the diode.

q: Electron charge.

n: Diode identity factor ($n = 1.3$).

N_s: Total number of photovoltaic cells connected in series.

T_n: Temperature at reference condition.

E_g: Energy band gap of the semiconductor material, approximately (≈1.1 eV).

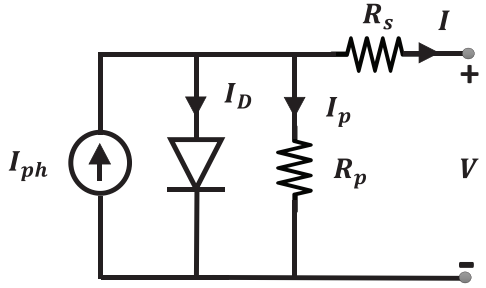

Figure 1: PV cell modeling using an equivalent circuit

Table 1: Specifications of the PV panel KC200GT in STC conditions

Power at MPP (W)	Current at MPP (A)	Voltage at MPP (V)	Short circuit current (A)	Open circuit voltage (V)	Number of cells in series	Number of cells in parallel
200	7.61	26.3	8.21	32.9	54	1

3 Modeling of Boost Converter

In photovoltaic application systems, the boost converter is widely used, particularly in MPPT controllers [17], as illustrated in Fig. 2. Assuming an ideal converter, the output voltage (V_0) is determined for a load resistance (R) of 36.12 Ω. As a result, both V_0 and the duty ratio (D) are calculated as follows:

$$V_0 = \sqrt{P_0 \times R} = 85V \tag{5}$$

$$D = 1 - \frac{V_{pv}}{V_0} = 0.69 \tag{6}$$

The inductor value is designed to achieve a 30% input current ripple (ΔI_{pv}) at a switching frequency of $f_s = 20$ kHz, while the output capacitor is sized to limit the output voltage ripple (ΔV_0) to 0.2%, as described in references [18,19], in order to minimize oscillations at MPP.

$$L = \frac{V_{pv} \times D}{2\Delta I_{pv} \times f_s} = 0.2 \text{ mH} \tag{7}$$

$$C = \frac{V_0 \times D}{2\Delta V_0 \times R \times f_s} = 240 \ \mu\text{F} \tag{8}$$

At 132 V, a practical capacitance of 300 µF is capable of supporting the output voltage of 85 V. To reduce the impact of equivalent series resistance, two capacitors are connected in parallel, resulting in an effective capacitance of C = 600 µF at 132 V.

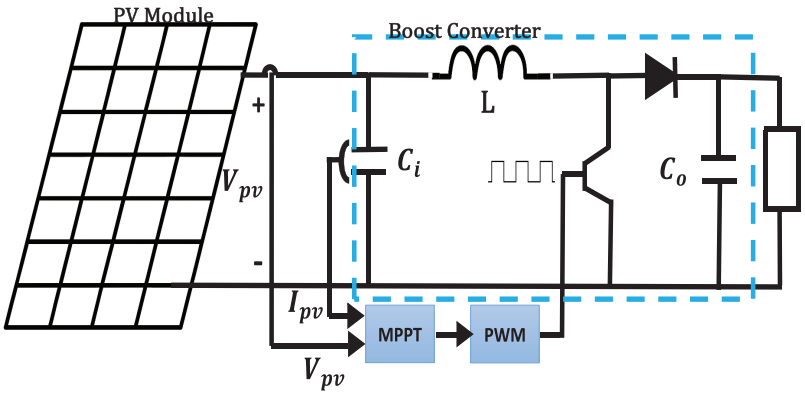

Figure 2: Boost converter with MPPT controller

4 MPPT Techniques

4.1 MPPT by Using Perturb and Observe

The P&O algorithm [20] determines the MPP by periodically adjusting the operating voltage of the PV generator and monitoring the corresponding change in output power. If an adjustment leads to an increase in power, the next step continues in the same direction. In contrast, a decrease in power causes the algorithm to reverse the direction of adjustment. Through this iterative process, the operating point gradually converges toward the MPP. The overall decision of our controller is shown in Fig. 3.

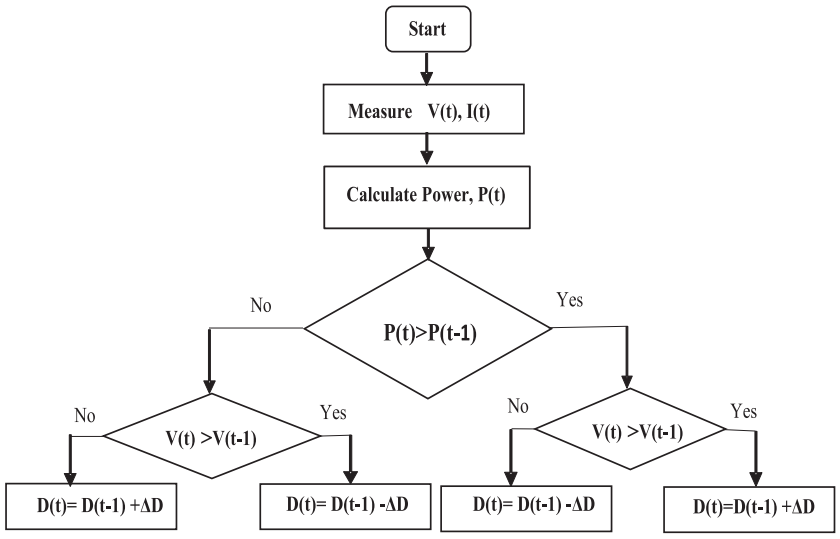

Figure 3: P&O flow chart

4.2 MPPT by Using Artificial Neural Networks

Artificial Neural Networks are a widely used artificial intelligence technique [21,22] with various applications, including PV energy conversion. For MPPT implementation, the ANN model shown in Fig. 4 establishes a nonlinear mapping between the input variables—solar irradiance and temperature—and the output signal that controls the DC/DC converter. For each change in irradiance or temperature, the ANN predicts the appropriate control action to maintain operation at the MPP.

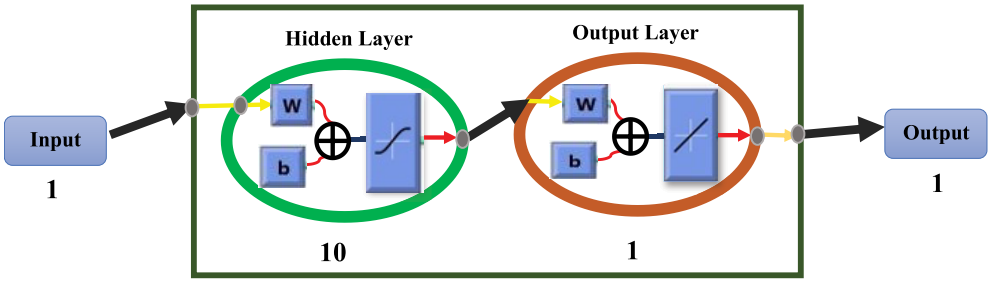

Figure 4: Architecture of the ANN based-MPPT controller

The model structure consists of a feedforward network with one hidden layer containing 10 neurons and an output layer with a single neuron, as illustrated in Fig. 5. The hidden layer employs a nonlinear activation function, while the output layer uses a linear function to provide the duty ratio. The network was trained using the Levenberg-Marquardt algorithm, which is well-suited for function approximation problems due to its fast convergence properties. The training dataset was constructed from combinations of irradiance and temperature values, covering a wide operating range to ensure robustness under varying environmental conditions.

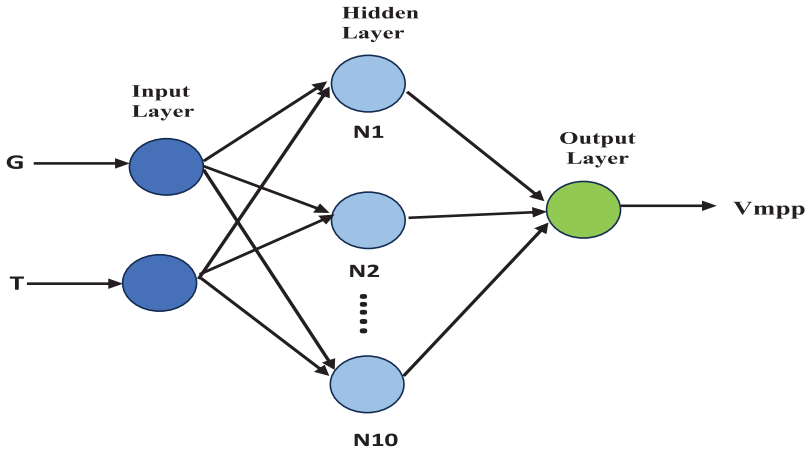

Figure 5: Structure of the ANN model for PV MPPT prediction

The performance of our ANN was evaluated using a dataset divided into training, validation, and testing subsets. Therefore, the mean squared error (MSE) decreased steadily over the training epochs, reaching its best validation performance of 3.8835×10^{-10} at epoch 1000, as shown in Fig. 6. The close overlap of the training, validation, and testing curves confirms that the model generalizes well without overfitting. This configuration ensures accurate and reliable prediction of the duty ratio, enabling efficient and stable MPPT operation.

4.3 MPPT by Using Incremental Conductance

Using the incremental conductance method [23,24], the PV generator's terminal voltage is determined by comparing and analyzing its incremental and instantaneous conductance. The discovery of the MPPT is indicated when the incremental conductance equals the instantaneous conductance. Fig. 7 illustrates the flow architecture of the INC controller.

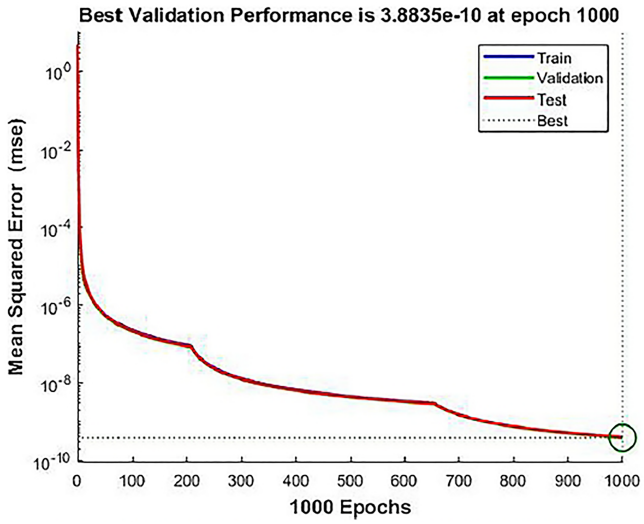

Figure 6: ANN performance evaluation in terms of MSE

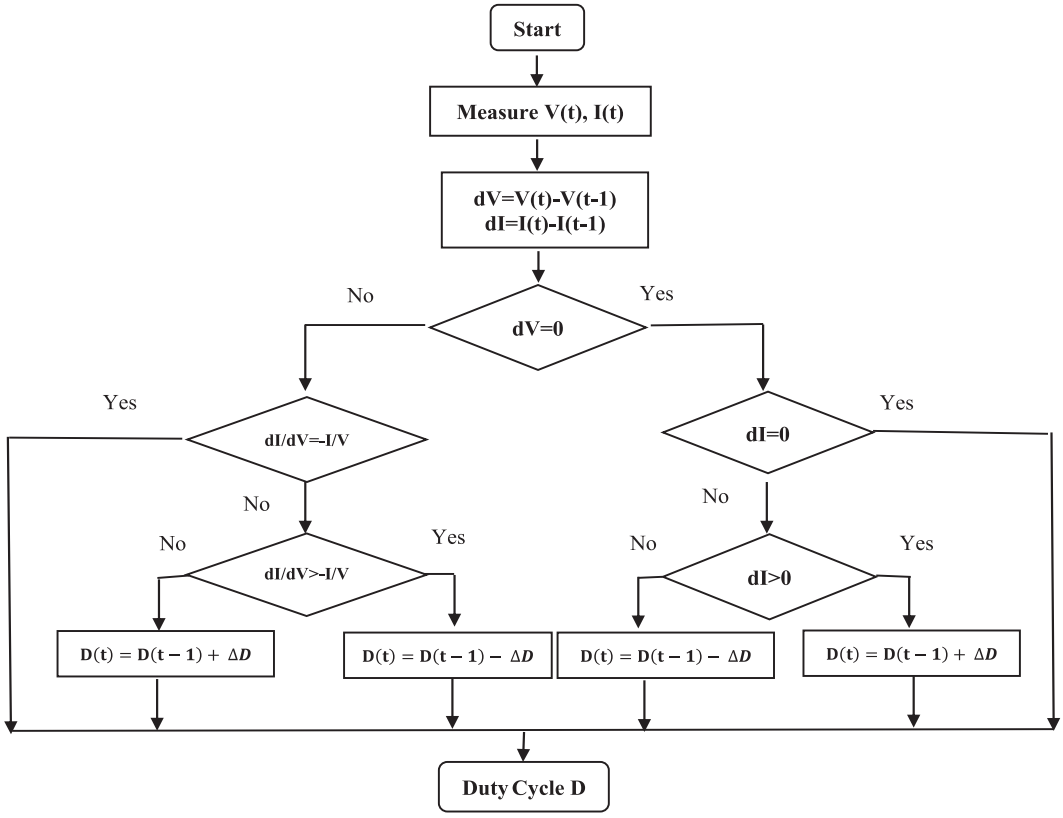

Figure 7: INC flow chart

4.4 MPPT by Using Fuzzy Logic

Fuzzy logic control is a method that enables the use of heuristic information obtained from expert knowledge to create nonlinear controllers [25]. A FL controller consists of several key components, as illustrated in Fig. 8. The input signals are first processed and converted into fuzzy values by the fuzzification block [26]. The rule base provides a linguistic representation of the variables to be controlled, based on a thorough understanding of the system. Using these rules and the corresponding membership functions, the inference engine interprets the data. The defuzzification block then converts the fuzzy outputs from the inference engine into crisp values, ensuring accurate process control. The rule-based structure of the fuzzy algorithm makes it easy to implement and independent of solar characteristics.

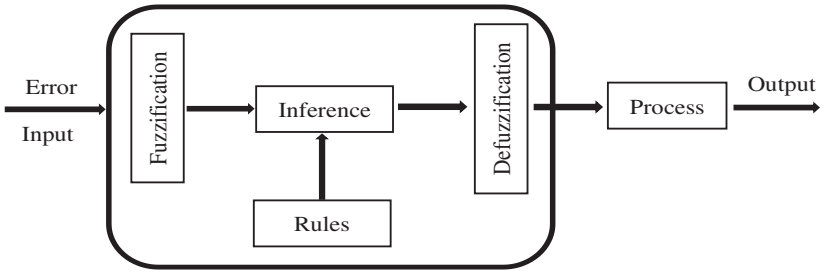

Figure 8: The key components of FL system

In our study, the formulation of the rule base was driven by the physical behavior of the photovoltaic system rather than by arbitrary choices. The controller uses two inputs: the error (E), which measures the distance from the MPP, and the change of error (ΔE), which reflects its temporal evolution. Both inputs were divided into seven linguistic levels, and the duty cycle adjustment was considered as the output, which was defined through these levels. This control operates as follows: when the error is largely positive, the duty cycle is sharply decreased. On the contrary, when the error is largely negative, it is increased. For small deviations, moderate adjustments are applied. Values close to zero result in minimal action to reduce oscillations. This systematic mapping ensures smooth transitions, robustness under rapid environmental fluctuations, and complete coverage of the operating domain. Table 2 summarizes the operational logic of the controller, which is based on 49 fuzzy control rules, and the linguistic variables are defined as follows: NS (Negative Small), NM (Negative Medium), NB (Negative Big), PS (Positive Small), PM (Positive Medium), PB (Positive Big), and Z (approximately zero).

The error (E) and the change in error (ΔE) are the two control variables used to determine which controls are chosen based on how well they are satisfied in the suggested input. We present the E and ΔE as follows:

$$E = \frac{P_n - P_{n-1}}{V_n - V_{n-1}} = \frac{\Delta P}{\Delta V} \tag{9}$$

$$\Delta E = E_n - E_{n-1} \tag{10}$$

The actual duty cycle ratio D is determined using the following formula:

$$D(j) = D(j-1) + S_{\Delta D}\Delta D(j) \tag{11}$$

Table 2: The rules implemented in the FLC

ΔE	NB	NM	NS	Z	PS	PM	PB
NB	NB	NB	NB	NM	NS	NS	Z
NM	NB	NB	NM	NM	NS	Z	PS
NS	NB	NM	NS	NS	Z	PS	PM
Z	NB	NM	NS	Z	PS	PM	PB
PS	NM	NS	Z	PS	PS	PM	PB
PM	NS	Z	PS	PM	PM	PB	PB
PB	Z	PS	PM	PB	PB	PB	PB

5 Results and Discussion

In our study, the proposed PV system was modeled and tested in MATLAB/Simulink using different MPPT techniques, as illustrated in Fig. 9. The PV system block represents the KC200GT PV module. The boost converter block is used to adapt the PV output voltage and ensure impedance matching with the load, thereby allowing optimal power transfer. The MPPT controller dynamically adjusts the duty cycle of the boost converter based on the measured PV voltage and current, ensuring maximal operating conditions. The load block models the electrical demand connected to the system, while the measurement and monitoring blocks provide signals such as power, current, and voltage for performance evaluation. To ensure the accuracy of the single diode representation of the panel, the simulated model was compared against the manufacturer's datasheet values under STC. Fig. 10 presents the P–V characteristics of the simulated KC200GT module in comparison with the datasheet reference, while Fig. 11 shows the corresponding I–V characteristics. The close agreement between the simulated and datasheet curves confirms the reliability of the adopted model, thereby providing a robust foundation for subsequent MPPT performance evaluation under varying irradiance and temperature conditions, and ensuring that the obtained results are both representative and meaningful for practical PV system behavior.

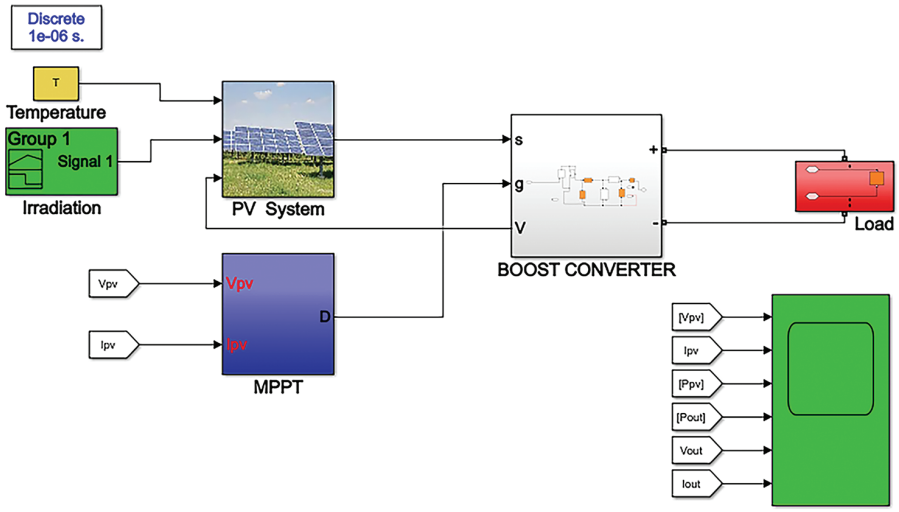

Figure 9: Proposed PV system with MPPT techniques

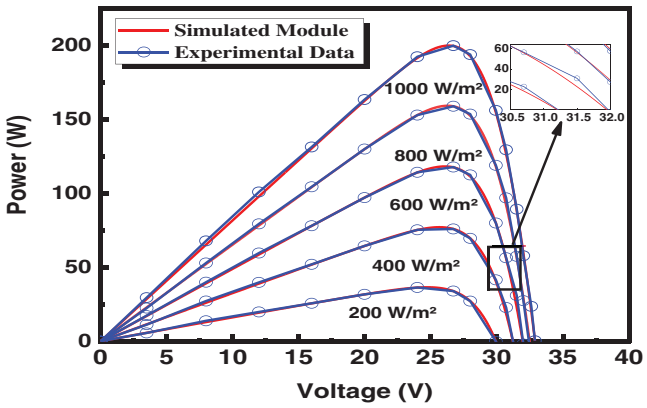

Figure 10: P–V characteristics of the simulated KC200GT module vs. datasheet values

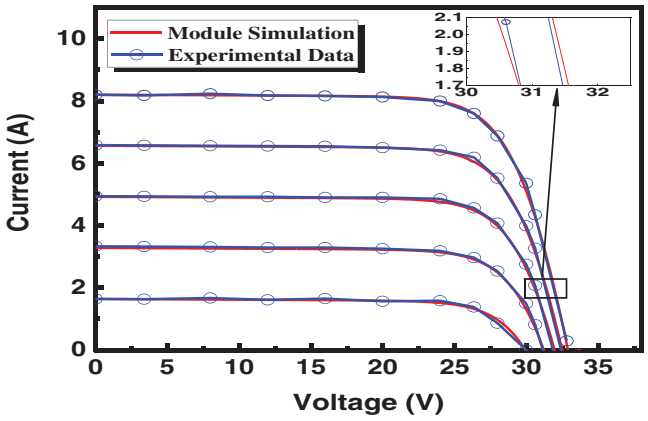

Figure 11: I–V characteristics of the simulated KC200GT module vs. datasheet values

Given that the performance of MPPT highly depends on both transient response and steady-state oscillations, a comparative analysis of the P&O, INC, FL, and ANN techniques was conducted under both constant and varying irradiance conditions. The detailed results, presented in Figs. 12–17, allow for a clear comparison in terms of tracking time, accuracy, and stability. Under STC, the Incremental Conductance method shows the slowest response, taking approximately 0.118 s to reach the MPP, with power oscillations in the range of 182.53 to 191.09 W. The Perturb and Observe method exhibits a very similar response time of 0.116 s with a fluctuation of 182.45 to 191.206 W. Considering that in both algorithms, the step size corresponds to the change of the converter duty cycle ΔD was set to 1×10^{-5} after a tuning process to achieve a compromise between convergence speed and steady state oscillations and it should be noted that the larger values of ΔD accelerate the tracking process but increase oscillations around the MPP, while smaller values reduce oscillations but make the response slower. Therefore, this choice ensures stable tracking with acceptable response time and efficiency, indicating nearly identical behavior in both dynamics and stability. The FL controller demonstrates the best performance, reaching the MPP in approximately 0.0585 s with a very narrow oscillation band (193.95–196.13 W), followed closely by the Artificial Neural Network, which reaches the MPP in 0.0587 s with limited fluctuations (192.56–194.32 W). However, although the ANN exhibits good speed and consistent stability, its efficiency decreases under low irradiance conditions, resulting in less accurate MPP tracking. The dynamic responses of all techniques are shown in Fig. 16, correlated

with the irradiance variations defined in Fig. 15, which confirms the superiority of the FL method, ensuring a fast transient response and remarkable stability in the face of sudden irradiance changes. The ANN maintains good consistency but shows reduced performance under low irradiance, while P&O and INC exhibit significant delays and pronounced oscillations during transitions. Therefore, the FL controller stands out as the most effective in terms of speed, accuracy, and overall stability, followed by the ANN, which remains competitive under high irradiance. In contrast, INC and P&O are less efficient, particularly in dynamic environmental conditions.

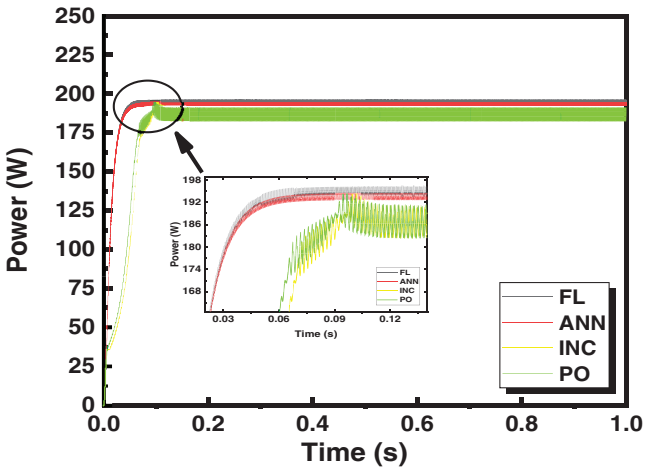

Figure 12: Output power of FL, INC and ANN controller

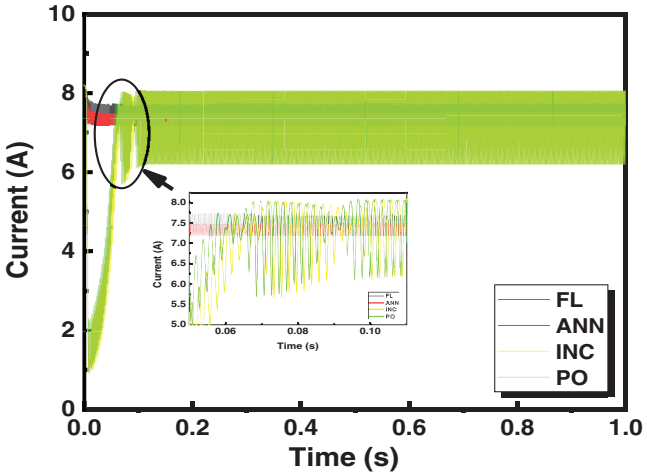

Figure 13: Output current of FL, INC, P&O and ANN technique

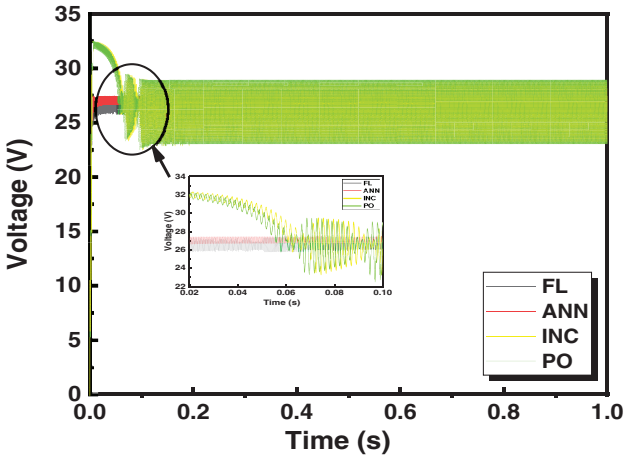

Figure 14: Output voltage of all the controlled methods

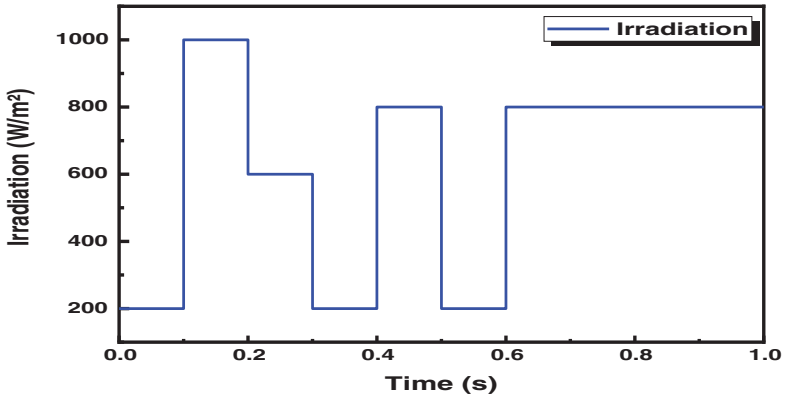

Figure 15: Variable Input irradiances of the PV system

Based on the performance results summarized in Table 3 below, which presents a statistical analysis of the four MPPT techniques under different irradiance levels, we aim to better evaluate the overall effectiveness and robustness of each method. The tracking efficiency at each irradiance is defined as:

$$\eta_i = \frac{P_{out,i}}{P_{the,i}} \tag{12}$$

To provide a more global assessment of the algorithms, the mean tracking efficiency and the standard deviation were calculated as:

$$\overline{\eta} = \frac{1}{N}\sum_{i=1}^{N}\eta_i \tag{13}$$

$$\sigma = \sqrt{\frac{1}{N-1}\sum_{i=1}^{N}(\eta_i - \overline{\eta})^2} \tag{14}$$

where $N = 5$ corresponds to the number of irradiance scenarios considered.

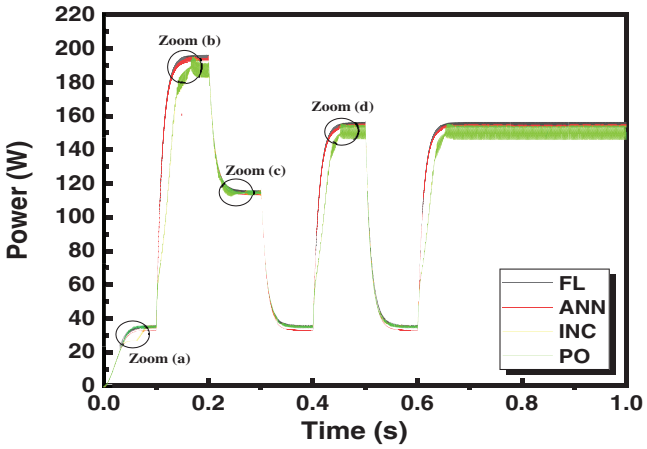

Figure 16: Output power of the tested model

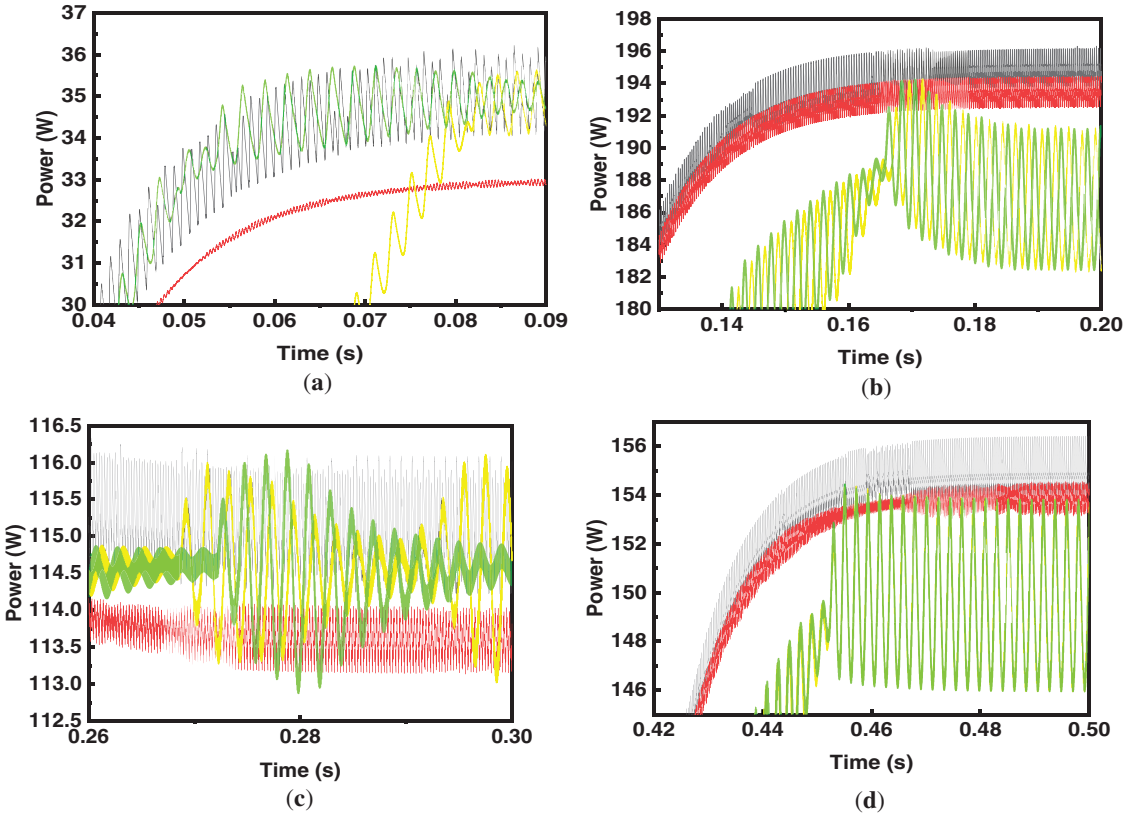

Figure 17: Zoomed views (**a**–**d**) of the PV output power under varying irradiance for FL, ANN, INC, and P&O MPPT techniques

The computed results are summarized in Table 4. As shown, the FL controller exhibits both the highest average efficiency and the lowest deviation, indicating strong robustness and stability across variations in irradiance. The ANN controller achieves a comparable mean efficiency but with a

significantly higher deviation, reflecting less consistent behavior, particularly at low irradiance levels. On the other hand, the P&O and INC methods yield similar mean efficiencies with moderate deviation, confirming their limited effectiveness.

Table 3: Performance analysis of all MPPT techniques at varying irradiance and fixed temperature (25°C)

Irradiance/ Temperature (W/m^2)/(°C)	Maximum theoretical power output $P_{the,i}$	Average instantaneous output power $P_{out,i}$				Power conversion efficiency η_i			
		FL	INC	ANN	P&O	FL	INC	ANN	P&O
1000/25	200	195.04	186.81	193.46	186.82	97.51%	93.39%	96.72%	93.40%
800/25	159.3	155.18	149.87	153.84	149,90	97.41%	94.08%	96.57%	94.10%
600/25	118.25	115.10	114.58	113.66	114.53	97.34%	96.90%	96.12%	96,85%
400/25	77.13	74.95	74.12	73.05	74.11	97.17%	96.10%	94.71%	96,08%
200/25	36.48	35.17	34.85	32.98	34.78	96.41%	95.53%	90.41%	95.34%

Table 4: Statistical evaluation of tracking efficiency across irradiance levels

MPPT technique mean	$\overline{\eta}$ (%)	σ standard deviation (%)
FL	97.17	0.44
ANN	94.91	2.64
P&O	95.15	1.41
INC	95.20	1.44

The computational complexity of the MPPT algorithms was estimated in terms of floating-point operations (FLOPs) by analyzing the number of basic arithmetic operations performed in the Simulink model at each sampling step. For consistency, additions and multiplications were counted as one FLOP, while divisions were considered more costly (≈8 FLOPs). Table 5 presents the estimated FLOP counts for each method. The results show that P&O requires the lowest number of operations, followed by INC, while FL incurs higher complexity due to the process of fuzzification, rule evaluation, and defuzzification. ANN has the highest computational demand, primarily because of multiple neuron weight multiplications and activation functions. These results indicate that advanced methods, such as FL and ANN, demand higher computational resources, regardless of their tracking performance, which must be taken into account for real-time implementation.

Table 5: Estimated computational complexity of MPPT algorithms in FLOPs per iteration

Technique	estimated FLOPs per iteration	Main sources of complexity
P&O	∼20 FLOPs	Voltage/current measurement, ΔP and ΔV calculation, duty cycle update
INC	∼35 FLOPs	Slope calculation (dI/dV), comparison, decision logic, duty cycle adjustment

(Continued)

Table 5 (continued)

Technique	estimated FLOPs per iteration	Main sources of complexity
FL	∼120 FLOPs	Fuzzification of 2 inputs, 49 rule evaluations, Mamdani inference, centroid defuzzification
ANN	∼200 FLOPs	Weighted sums (input × weights), bias addition, activation functions, output computation

In addition to the performance evaluation, it is important to consider the implementation feasibility of the investigated algorithms. The P&O and INC techniques remain attractive due to their simplicity, low processing requirements, and ease of deployment on inexpensive microcontrollers, even if their efficiency can fluctuate under dynamic conditions. ANN and FL controllers demand more memory, design effort, and computational resources, which may increase their hardware cost and complexity. However, these advanced methods can provide greater flexibility and an ability to handle with nonlinear system behavior, provided that the ANN is trained on a sufficiently rich and representative dataset that includes both low irradiance and dynamic scenarios, and that the FL membership functions, scaling factors and rule base are correctly specified and validated, under these conditions, they become suitable for integration on more powerful digital platforms. Therefore, the choice of the MPPT algorithm should strike a balance between measured efficiency and computational complexity, as well as implementation costs.

6 Conclusion

Overall, while the FL controller has shown superior performance and robustness in our study, it should not be interpreted as a universally dominant solution; each algorithm exhibits specific strengths and weaknesses that depend on the operating conditions. The ANN performs very well under high irradiance, but its degradation at lower irradiance suggests that our future work should focus on improving training datasets, including more diverse low-irradiance scenarios, or integrating adaptive retraining mechanisms. Additionally, the primary limitation of the FL controller is its reliance on expert-designed rules and membership functions, which can limit its scalability across different PV technologies. To overcome this constraint, we can use adaptive or self-tuning fuzzy systems. On the other hand, INC and P&O are more stable at low irradiance than ANN, but still exhibit slower convergence and oscillations around the MPP.

Therefore, our future study should emphasize the importance of considering hybrid or adaptive MPPT strategies that combine the robustness of FL, the learning capability of ANN, and the simplicity of INC and P&O. Additionally, it should incorporate partial shading conditions and real-world experimental validations to confirm the reliability of these approaches under practical deployment scenarios.

Acknowledgement: The author would like to thank the Higher School of Technology–Guelmim (ESTG), Morocco, for providing access to high-performance computing facilities. The author expresses sincere gratitude to ESTG for the logistical and technical support provided throughout this research.

Funding Statement: The author received no specific funding for this work. The Article Processing Charge (APC) was funded by the author.

Author Contributions: The authors confirm contribution to the paper as follows: Conceptualization, methodology, writing—original draft preparation, Kamal Boujaghama; investigation, supervision, validation, Naoufel Khaldi; project administration, supervision, Rachid Markazi; investigation, writing—review and editing, Lahcen Amhaimar. All authors reviewed the results and approved the final version of the manuscript.

Availability of Data and Materials: The data that support the findings of this study are available from the corresponding author, Kamal Boujaghama, upon reasonable request.

Ethics Approval: Not applicable.

Conflicts of Interest: The authors declare no conflicts of interest to report regarding the present study.

References

1. Gorjian S, Sharon H, Ebadi H, Kant K, Scavo FB, Tina GM. Recent technical advancements, economics and environmental impacts of floating photovoltaic solar energy conversion systems. J Clean Prod. 2021;278:124285. doi:10.1016/j.jclepro.2020.124285.
2. Ashwini M, Basha CH, Alraddadi M, Alsaif F, Irfan MM. Design and comprehensive analysis of adjustable step MPPT controllers for solar PV systems under stochastic atmospheric conditions. Sci Rep. 2025;15(1):10369. doi:10.1038/s41598-025-95136-1.
3. Kannan N, Vakeesan D. Solar energy for future world:—a review. Renew Sustain Energ Rev. 2016;62(1):1092–105. doi:10.1016/j.rser.2016.05.022.
4. Slimi M, Boucheta A, Bouchiba B. Maximum power control for photovoltaic system using intelligent strategies. Int J Power Electron Drive Syst. 2019;10:423–32. doi:10.11591/ijpeds.v10.i1.pp423-432.
5. Abdullah MZ, Sudiharto I, Eviningsih RP. Photovoltaic system MPPT using fuzzy logic controller. In: 2020 International Seminar on Application for Technology of Information and Communication; 2020; Semarang, Indonesia. p. 378–83.
6. Jyothy LPN, Sindhu MR. An artificial neural network based MPPT algorithm for solar PV system. In: 2018 4th International Conference on Electrical Energy Systems; 2018; Chennai, India. p. 375–80.
7. Alzahrani A. A fast and accurate maximum power point tracking approach based on neural network assisted fractional open-circuit voltage. Electronics. 2020;9(12):2206. doi:10.3390/electronics9122206.
8. Zeynal H, Zakaria Z, Pourveis B. An efficient MPPT based photovoltaic control model considering environmental parameters. Int J Power Electron Drive Syst. 2022;13(4):2432–9. doi:10.11591/ijpeds.v13.i4.pp2432-2439.
9. Bahari MI, Tarassodi P, Naeini YM, Khalilabad AK, Shirazi P. Modeling and simulation of hill climbing MPPT algorithm for photovoltaic application. In: International Symposium on Power Electronics, Electrical Drives, Automation and Motion; 2016; Capri, Italy. p. 1041–4. doi:10.1109/speedam.2016.7525990.
10. Husain MA, Pingale SB, Bakar Khan A, Faiz Minai A, Pandey Y, Shyam Dwivedi R. Performance analysis of the global maximum power point tracking based on spider monkey optimization for PV system. Renew Energy Focus. 2023;47(2):100503. doi:10.1016/j.ref.2023.100503.
11. Pai F-S, Tseng P-S. An efficient GWO MPPT for a PV system using impedance information acceleration. Int J Electron. 2019;106(4):648–61. doi:10.1080/00207217.2018.1545929.

12. Badea A-M, Manaila-Maximean D, Fara L, Craciunescu D. Maximizing solar photovoltaic energy efficiency: MPPT techniques investigation based on shading effects. Sol Energy. 2025;285(1):113082. doi:10.1016/j.solener.2024.113082.
13. Naseem M, Husain MA, Minai AF, Khan AN, Amir M, Dinesh Kumar J, et al. Assessment of meta-heuristic and classical methods for GMPPT of PV system. Trans Electr Electron Mater. 2021;22:217–34. doi:10.1007/s42341-021-00306-3.
14. Yousaf MZ, Khalid S, Tahir MF, Tzes A, Raza A. A novel dc fault protection scheme based on intelligent network for meshed dc grids. Int J Electrical Power Energy Syst. 2023;154(3):109423. doi:10.1016/j.ijepes.2023.109423.
15. Yousaf MZ, Liu H, Raza A, Mustafa A. Deep learning-based robust DC fault protection scheme for meshed HVDC Grids. CSEE J Power Energy Syst. 2023;9:2423–34. doi:10.17775/CSEEJPES.2021.03550.
16. Senthilkumar S, Mohan V, Mangaiyarkarasi SP, Karthikeyan M. Analysis of single-diode PV model and optimized MPPT model for different environmental conditions. Int Trans Electr Energy Syst. 2022;2022(3):4980843–17. doi:10.1155/2022/4980843.
17. Fathi M, Parian JA. Intelligent MPPT for photovoltaic panels using a novel fuzzy logic and artificial neural networks based on evolutionary algorithms. Energy Rep. 2021;7(31):1338–48. doi:10.1016/j.egyr.2021.02.051.
18. Manna S, Singh DK, Akella AK, Kotb H, AboRas KM, Zawbaa HM, et al. Design and implementation of a new adaptive MPPT controller for solar PV systems. Energy Rep. 2023;9(16):1818–29. doi:10.1016/j.egyr.2022.12.152.
19. Hashim N, Salam Z, Johari D, Nik Ismail NF. DC-DC boost converter design for fast and accurate MPPT Algorithms in stand-alone photovoltaic system. IJPEDS. 2018;9(3):1038. doi:10.11591/ijpeds.v9.i3.pp1038-1050.
20. Ahmed J, Salam Z. An enhanced adaptive P&O MPPT for fast and efficient tracking under varying environmental conditions. IEEE Trans Sustain Energy. 2018;9(3):1487–96. doi:10.1109/TSTE.2018.2791968.
21. Villegas-Mier CG, Rodriguez-Resendiz J, Álvarez-Alvarado JM, Rodriguez-Resendiz H, Herrera-Navarro AM, Rodríguez-Abreo O. Artificial neural networks in MPPT algorithms for optimization of photovoltaic power systems: a review. Micromachines. 2021;12(10):1260. doi:10.3390/mi12101260.
22. Khaldi N, Mahmoudi H, Zazi M, Barradi Y. The MPPT control of PV system by using neural networks based on Newton Raphson method. In: 2014 International Renewable and Sustainable Energy Conference; 2014; Ouarzazate, Morocco. p. 19–24.
23. Mohamed SA, Abd El Sattar M. A comparative study of P&O and INC maximum power point tracking techniques for grid-connected PV systems. SN Appl Sci. 2019;1:174.
24. Mokhlis M, Ferfra M, Vall HA, idrissi RE, Ahmed CC, Taouni A. Comparative study between the different MPPT techniques. In: 5th International Conference on Renewable Energies for Developing Countries; 2020; Marrakech, Morocco. p. 1–6.
25. Tang HH, Ahmad NS. Fuzzy logic approach for controlling uncertain and nonlinear systems: a comprehensive review of applications and advances. Syst Sci Control Eng. 2024;12:2394429.
26. Cheng P-C, Peng B-R, Liu Y-H, Cheng Y-S, Huang J-W. Optimization of a fuzzy-logic-control-based MPPT algorithm using the particle swarm optimization technique. Energies. 2015;8(6):5338–60. doi:10.3390/en8065338.